Static analysis of interaction between two adjacent top tensioned risers with consideration of wake effects

Deqiang Tian[a], Honghai Fan[a], Bernt J Leira[b], Svein Sævik[b], Ping Fu[a]

[a] College of Petroleum Engineering, China University of Petroleum-Beijing, Beijing, 102249, China
[b] Department of Marine Technology, Norwegian University of Science and Technology, Trondheim, 7052, Norway

ABSTRACT

Collision between adjacent risers has become an important issue as the oil and gas industry moves to deeper waters. In order to estimate the clearance between two marine risers, a static analysis which is mainly concerned with the wake effects is performed in this paper. A new wake model, which is used to predict the wake flow around the downstream riser, is developed based on Prandtl's shearing stress hypothesis. The wake effects with respect to riser interference in uniform current flow are then investigated. In this work, the two risers are both simplified as circular cylinders top-tensioned and pinned at the bottom. A procedure for iteratively predicting the wake velocity distribution and estimating the clearance between two risers is introduced to find the final convergent result by combining the new wake model with the global riser analysis software Riflex. The effects of different factors like riser spacing, top tension force and current velocity are also studied. The results indicate that these factors significantly influence the riser interference. Since the current velocity cannot in general be controlled for a specific site, the riser spacing and the top tension force become the primary design parameters that can be chosen by the operator.

1. Introduction

Marine risers play crucial roles in global offshore exploration, installation and production activities. Due to economical and practical considerations, drilling and production risers on offshore platforms are commonly arranged in clusters with relatively close spacing. Riser collision is therefore more likely to occur for such compact arrangements than for more sparse system layouts. This is illustrated in Fig. 1-a. Specifically, wake interference plays an important role for assessment of the potential for collision between two risers, which takes place when a downstream riser is located in the wake field of an upstream riser pipe. The wake interference will change the flow around the downstream riser, i.e. reducing the local flow velocity, and, consequently reduce the associated drag force. This will also induce an additional lift force if the risers are arranged in a staggered configuration. This effect in turn decreases the clearance between the adjacent risers and will accordingly imply a potential for collision between them. This is illustrated by Fig. 1-b.

Commonly, there are two different design strategies for riser collision assessment according to DNV-RP-F203 (2009). One is called 'No Collision Allowed', which means that riser collision is not allowed under normal, extreme or survival conditions. Another one is 'Collision Allowed', which allow infrequent riser collision in some extreme conditions. For the latter strategy, although riser collision is unlikely to lead to a sudden failure, one potential risk is that it can initiate the onset of fatigue failure from a long term point of view (Fu et al., 2017). So, for the present study, a static analysis and clearance assessment based on the former strategy is considered in order to avoid riser collision and to prolong the operational lifetime of the risers.

This work is motivated by the industry need for effective toolkit to support design analysis of Top Tensioned Risers (TTRs), which represent a crucial part of offshore facilities. Accurate prediction of wake interference can help to produce more robust structural design and lead to substantial savings in relation to offshore applications.

The problem of wake effects is addressed by different approaches, which roughly can be categorized into one of three major groups: experiments, Computational Fluid Dynamics (CFD) and analytical models. During the last three decades, significant advances have been made with respect to CFD and experimental studies (Assi et al., 2006; Kang, 2003; Sagatun et al., 2002; Sumner et al., 1999; Zdravkovich, 1987) in relation to wake interference between risers. A comprehensive literature review of these studies can be found in Sumner (2010). In contrast, substantially less efforts have been made in order to investigate analytical wake

Nomenclature

ε_o, C	constants
x	streamwise distance
y	transverse distance
C_{Du}, C_{Dd}	the drag coefficient of upstream and downstream riser
F_{Du}, F_{Dd}	the drag force on upstream and downstream riser
D_u, D_d	the diameter of upstream and downstream riser
h	length of riser
U_∞	free-stream velocity
u	Time-averaged streamwise wake velocity
v	Time-averaged transverse wake velocity
$\overline{u}$	deficit velocity
$\overline{u}_1$	the first term of deficit velocity
Re	Reynolds number
$\overline{u}_2$	the second term of deficit velocity
$\overline{u}_n$	the n *th* term of deficit velocity
v_1	the first term of transverse velocity
v_2	the second term of transverse velocity
ρ	density of fluid
υ	laminar kinematic viscosity of fluid
p	Time-averaged hydrostatic pressure
ε_τ	virtual kinematic viscosity
κ_1	Empirical constant
b	the width of the mixing zone
$P\ (x_0, y_0)$	any point in downstream wake area
R^2	Coefficient of determination
L, T	Riser spacing and top tension coefficient

models which are of great significance to offshore engineering. Analytical wake models are represented by numerous approaches in order to model the wake field, with some of them incorporating the boundary layer equation as the governing analysis component.

With respect to theoretical analysis, Tollmien and Miner (1931) considered the problem of finding the first approximation to the asymptotic form of the two-dimensional wake field far behind a flat plate. Goldstein (1933) found the next approximation to the far-wake solution of Tollmien based on the Ossen approximation. The nature of two-dimensional wakes behind circular cylinder were first studied by Schlichting and Gersten (1979), who solved the equations of motion in a wake by use of different mixing theories after L. Prandtl. By assuming two-dimensional motion, neglecting viscous stress and holding the pressure constant through the fluid, Schlichting set up an expression to describe the wake behind a cylinder. The expression is found to be in good agreement with experimental data. However, this solution just constituted an approximation which is only valid for very large distances behind the cylinder, i.e. $x/(C_D \cdot d) > 50$. Close to the upstream cylinder, the expression will give a wake peak which is quite high and narrow and will lead to erroneous results when trying to calculate the force acting on a second body placed in the wake. Another analytical model proposed by Reichardt (1941) expresses the deficit velocity behind a circular cylinder as a function of the distance from the center, which also gives good agreement with the experimental data in the far field wake (Schlichting and Gersten, 1979).

It is noticed that the analytical model respectively presented by Schlichting and Reichardt is tailored to circular cylinder and only valid for far wake investigation. Huse and Muren (1987) first applied the wake model to the problem of marine riser interaction. Later, the semi-empirical approach to wake effect was further studied by Huse (1992) who modified Reichardt's model by assuming that the wake field behind a circular cylinder is generated by a 'virtual source' which is located at the upstream of the first cylinder. This is known as the Huse wake model. Blevins (2005) developed a method by introduction of mean drag- and lift force on the downstream riser as a function of the relative distance between two risers. The Reichardt's expression of deficit velocity at the cylinder center is directly used in the Blevins model, with the assumption that the drag force on the downstream cylinder in the wake is proportional to the local dynamic pressure evaluated at its center. The Blevins model can be regarded as a transformation of Reichardt's model but with different constants which are obtained by correlating Price's (1975); Price and Paidoussis (1984) experimental data within the framework of Reichardt's model.

Currently, the Huse model and the Blevins model are the most commonly used wake model for analysis in relation to riser interference. Wu et al. (2002) investigated the mean lift and drag forces on a cylinder placed in the wake of another upstream cylinder as well as the influence of these forces on the stability of the downstream cylinder, and the Huse model was used to determine the wake field. Huang (2010) studied the instability of a vertical riser in the wake of an upstream vertical riser by

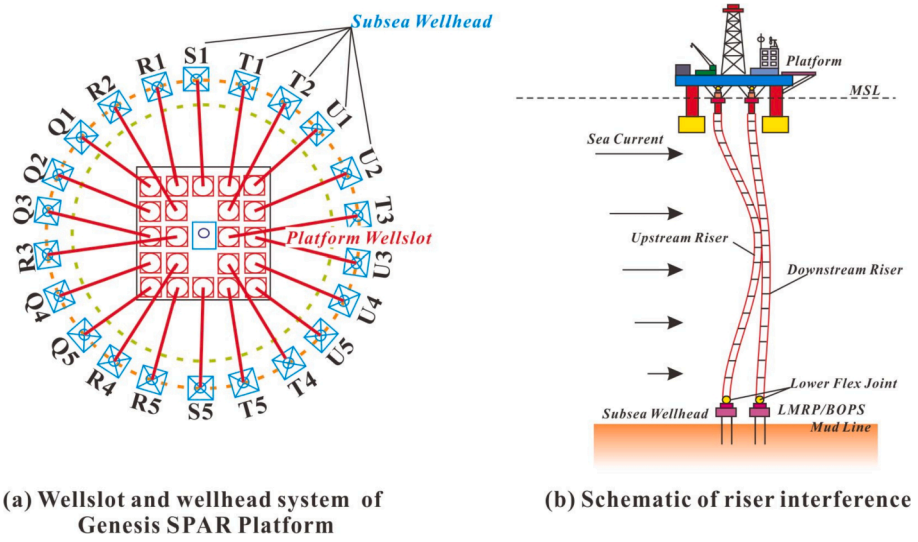

(a) Wellslot and wellhead system of Genesis SPAR Platform

(b) Schematic of riser interference

Fig. 1. Example of wellslot and wellhead system and schematics of riser interference.

using the Huse model to estimate the mean wake flow velocity at the downstream riser. In the works by Fu et al. (2017) and Fu et al. (2018), the Huse model and the Blevins model were both used to investigate the collision probability for flexible risers subjected to current and waves. Existing tools for riser analysis like OrcaFlex and Flexcom are still using the Huse model and the Blevins model as the major analytical models to support riser interference analysis.

In spite of these significant research efforts in relation to analytical wake models, more work is still required within this area. The 'virtual source position' introduced in the Huse model is basically given based on engineering experiences but with an insufficient theoretical foundation, which leads to the estimated results being amplified in the near wake. As the Blevins model is directly derived from the Reichardt model, the deficit of Reichardt model is not eliminated. Moreover, the parameters in the Blevins model are obtained by fitting the Reichardt's formula only with Price's published data. This makes the Blevins model possibly invalid when the temporal conditions are significantly different from the Price's experimental data. Therefore in this paper we propose a new effective wake model which is intended to fill this gap.

The rest of the paper is organized as follows. In the next section the traditional models are briefly introduced and compared. Subsequently, the new wake model is developed. Here it is shown how the mean wake velocity is deduced from the boundary layer equations by using Tollmien's first approximation method and Goldstein's second approximation method. The model is then calibrated using different published experimental data and CFD results. In the subsequent section, a detailed procedure for predicting the wake velocity distribution and estimating the clearance between two marine risers iteratively is introduced in order to find the final static displacement of the two risers. The fluid forces are calculated using the Morison equation. The lift force acting on the downstream riser is neglected due to the risers being arranged in tandem. A case study is performed by incorporating the new wake model into the global riser analysis software Riflex (SINTEF, 2017). Special attention is paid to the effect of wake models on the static analysis results and the sensitivity factors with respect to riser systems are also investigated. Finally, some concluding remarks are given.

2. Wake interference

2.1. The Huse model

According to Reichardt (1941), the local flow velocity behind a cylinder can be expressed as:

$$u(x,y)=U_\infty\cdot\left\{1-0.95\cdot\sqrt{\frac{C_{Du}\cdot D_u}{x}}\cdot exp\left\{-\frac{y^2}{0.08888C_{Du}\cdot D_u\cdot x}\right\}\right\} \tag{1}$$

where $u(x,y)$ is the time-averaged local flow velocity in the wake field, U_∞ is the free-stream velocity, C_{Du} is the drag coefficient based on free-stream velocity, D_u is the diameter of the upstream cylinder. The origin of the local coordinate system is located at the center of the cylinder, with the x-axis pointing the incoming flow direction, and the y-axis in the transverse direction.

Huse (1992) proposed a concept of 'vitural source' to improve Reichardt's formula. In Huse's opinion, the wake field generated by a circular cylinder can approximately be replaced by a 'virtual' cylinder located at somewhere upstream of the real cylinder. The center of the virtual cylinder, namely the virtual source, is located at x_v away in front of the center of the real cylinder, where $x_v = 4D_u/C_{Du}$. This definition make sure that the wake width at the real cylinder center is exactly equal to the cylinder diameter. Hence the local flow velocity $u(x,y)$ can be determined by using the modified distance $x_s = x + x_v$ instead of x in Eq. (1), which can be expressed as:

$$u(x,y)=U_\infty\cdot\left\{1-\sqrt{\frac{C_{Du}\cdot D_u}{x+4D_u/C_{Du}}}\cdot exp\left\{\frac{-11.26y^2}{C_{Du}\cdot D_u\cdot(x+4D_u/C_{Du})}\right\}\right\} \tag{2}$$

It should be noticed that some constants are changed compared with Eq. (1).

2.2. The Blevins model

Blevins (2005) pointed out that the drag force on a cylinder in a wake is proportional to the local dynamic pressure evaluated at its center. Therefore the variation of the local flow velocity behind a cylinder can be translated to the variation of the drag coefficient of the downstream riser, which can be expressed as:

$$\begin{aligned}F_{Dd}&=\frac{1}{2}\cdot\rho\cdot D_d\cdot C_{Ddo}\cdot u(x,\ y)^2=\frac{1}{2}\cdot\rho\cdot D_d\cdot C_{Ddo}\cdot U_\infty^2\cdot\left[\frac{u(x,\ y)}{U_\infty}\right]^2\\&=\frac{1}{2}\cdot\rho\cdot D_d\cdot U_\infty^2\cdot C_{Dd}(x,\ y)\end{aligned} \tag{3}$$

so,

$$C_{Dd}(x,\ y)=C_{Ddo}\cdot[u(x,\ y)/U_\infty]^2 \tag{4}$$

where C_{Ddo} is the reference drag coefficient for the downstream cylinder in the free stream velocity U_∞, $C_{Dd}(x,\ y)$ is the downstream cylinder drag coefficient based on its local flow velocity $u(x,y)$.

Inserting Eq. (1) into Eq. (4) this becomes:

$$C_{Dd}(x,\ y)=C_{Ddo}\cdot\left\{1-a_1\left(\sqrt{\frac{C_{Du}\cdot D_d}{x}}\right)\cdot exp\left\{-\frac{a_2y^2}{C_{Du}\cdot D_d\cdot x}\right\}\right\}^2 \tag{5}$$

where $a_1 = 1$, $a_2 = 4.5$ are determined by fitting method as mentioned in the previous section.

The Blevins model also contains the expression of the inward lift force on the downstream cylinder, see Eq. (6), towards the wake center-line, which is proportional to the transverse gradient of the drag force. In the present study, the downstream riser is placed at the wake center-line. Then, the lift force on the downstream riser can be neglected, since the lift force is equal to zero when inserting y = 0 into Eq. (6).

$$\begin{aligned}C_{Ld}(x,\ y)=a_3\left(\frac{yC_{Ddo}D_d}{xC_{Du}D_u}\right)\sqrt{\frac{C_{Du}\cdot D_u}{x}}\cdot\left\{1-a_1\sqrt{\frac{C_{Du}\cdot D_u}{x}}\right.\\\left.\times\ exp\left[-\frac{a_2y^2}{C_{Du}\cdot D_u\cdot x}\right]\right\}exp\left[-\frac{a_2y^2}{C_{Du}\cdot D_u\cdot x}\right]\end{aligned} \tag{6}$$

where $a_3 = -10.6$, $C_{Ld}(x,\ y)$ is the lift coefficient based on its local flow velocity $u(x,y)$.

2.3. Second approximation based wake model

All wake models described so far are deduced through Blasiu' method which only gives a first approximation solution for large x. In this subsection, a new wake model is developed by a second approximation method aims at improving the prediction of the wake in the intermediate field between the very near wake and the far wake. A schematic layout of the two-dimensional wake flow downstream of a riser with outside diameter d is shown in Fig. 2.

The free-stream velocity of the steady flow U_∞ is assumed to be expressed as:

$$U_\infty = u(x,y) + \overline{u}(x,y) \tag{7}$$

where $u(x,y)$ and $\overline{u}(x,y)$ are the time-averaged wake velocity and the deficit velocity at any point P $(x,\ y)$ in the downstream wake area, respectively.

As stated by Schlichting and Gersten (1979), in the case of steady

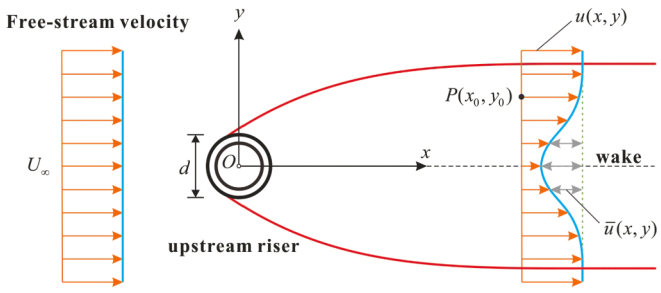

Fig. 2. Sketch of wake model.

flow, the Prandtl's boundary-layer equations can be simplified into:

$$\begin{cases} -\dfrac{\partial \bar{u}}{\partial x}+\dfrac{\partial v}{\partial y}=0 \\ -U_\infty \dfrac{\partial \bar{u}}{\partial x}+\upsilon \dfrac{\partial^2 \bar{u}}{\partial y^2}=-\bar{u}\dfrac{\partial \bar{u}}{\partial x}+v\dfrac{\partial \bar{u}}{\partial y} \end{cases} \tag{8}$$

with the following boundary conditions:

$$y=0: u=v=0; \quad y=\infty: u=U_\infty \tag{9}$$

where v is the time-averaged transverse wake velocity; υ is the laminar kinematic viscosity of the fluid. The pressure distribution is assumed to be constant in the downstream flow.

According to Tollmien's (1931) first approximation method and Goldstein's (1933) second approximation method, an iteration scheme is then set up in which the *n th* term is related to the *(n-1)th* approximation by the equations:

$$\begin{cases} -\dfrac{\partial \bar{u}_n}{\partial x}+\dfrac{\partial v_n}{\partial y}=0 \\ -U_\infty \dfrac{\partial \bar{u}_n}{\partial x}+\upsilon \dfrac{\partial^2 \bar{u}_n}{\partial y^2}=-\bar{u}_{n-1}\dfrac{\partial \bar{u}_{n-1}}{\partial x}+v_{n-1}\dfrac{\partial \bar{u}_{n-1}}{\partial y} \end{cases} \tag{10}$$

where the velocity components are given by: $\bar{u}=\bar{u}_1+\bar{u}_2+\cdots+\bar{u}_n$, $\bar{v}=\bar{v}_1+\bar{v}_2+\cdots+\bar{v}_n$, $\bar{u}_0=v_0=0$. By keeping the terms up to the second order, the following is obtained:

$$\bar{u}\approx\bar{u}_1+\bar{u}_2 \tag{11}$$

Eq. (10) can be written as Eq. (12) when $n=1$:

$$\begin{cases} -\dfrac{\partial \bar{u}_1}{\partial x}+\dfrac{\partial v_1}{\partial y}=0 \\ U_\infty \dfrac{\partial \bar{u}_1}{\partial x}=\upsilon \dfrac{\partial^2 \bar{u}_1}{\partial y^2} \end{cases} \tag{12}$$

with the boundary conditions:

$$y=0: \frac{\partial \bar{u}_1}{\partial y}=0; \quad y=\infty: \bar{u}_1=0 \tag{13}$$

The expression for the first term of the deficit velocity $\bar{u}_1$ can then be expressed as in Eq. (14) by solving Eq. (12), with more details of the solution process being shown in Appendix A.

$$\frac{\bar{u}_1}{U_\infty}=\alpha\cdot C_D^{1/2}\cdot\left(\frac{x}{d}\right)^{-1/2}\cdot exp\left\{-4\pi\alpha^2\cdot C_D^{-1}\cdot\left(\frac{x}{d}\right)^{-1}\cdot\left(\frac{y}{d}\right)^2\right\} \tag{14}$$

For the second approximation, i.e. corresponding to n = 2, Eq. (10) is expressed as:

$$\begin{cases} -\dfrac{\partial \bar{u}_2}{\partial x}+\dfrac{\partial v_2}{\partial y}=0 \\ -U_\infty \dfrac{\partial \bar{u}_2}{\partial x}+\varepsilon_o \dfrac{\partial^2 \bar{u}_2}{\partial y^2}=-\bar{u}_1\dfrac{\partial \bar{u}_1}{\partial x}+v_1\dfrac{\partial \bar{u}_1}{\partial y} \end{cases} \tag{15}$$

The expression for the second term of the deficit velocity $\bar{u}_2$ can be expressed by Eq. (16) which is obtained by solving Eq. (15). More details of the solution process is shown in Appendix B.

$$\frac{\bar{u}_2}{U_\infty}=\frac{\alpha^2}{2}C_D\left(\frac{x}{d}\right)^{-1}\cdot exp\left\{-4\pi\alpha^2\beta\cdot C_D^{-1}\cdot\left(\frac{x}{d}\right)^{-1}\cdot\left(\frac{y}{d}\right)^2\right\} \tag{16}$$

The expression for the time-averaged streamwise wake velocity is then given on the following form by combining Eq. (7), (11), (14), (16):

$$\begin{aligned} \frac{u}{U_\infty}&=1-\frac{\bar{u}_1}{U_\infty}-\frac{\bar{u}_2}{U_\infty} \\ &=1-\alpha\cdot C_D^{1/2}\cdot\left(\frac{x}{d}\right)^{-1/2}\cdot exp\left\{-4\pi\alpha^2\cdot C_D^{-1}\cdot\left(\frac{x}{d}\right)^{-1}\cdot\left(\frac{y}{d}\right)^2\right\} \\ &\quad-\frac{\alpha^2}{2}\cdot C_D\cdot\left(\frac{x}{d}\right)^{-1}\cdot exp\left\{-4\pi\alpha^2\beta\cdot C_D^{-1}\cdot\left(\frac{x}{d}\right)^{-1}\cdot\left(\frac{y}{d}\right)^2\right\} \end{aligned} \tag{17}$$

Eq. (17) is fitted to published numerical and experimental wake velocity distribution data in order to optimize the value of the coefficients α and β. The results are $\alpha=0.55$, $\beta=8.3$. At large distances, this applied second order approximation method does not make much difference when calculating the wake field. However, it makes a significant difference for the wake field in the proximity of the upstream riser.

2.4. Calibration and discussion

In order to validate the presented model, comparison is made with published results that are obtained by means of both numerical (Breuer, 2000; Kravchenko and Moin, 2000; Richter et al., 2012; Prsic et al., 2014) and experimental (Cantwell and Coles, 1983; Lyn et al., 1995; Lourenco and Shih, 1993) methods. Marine risers are subjected to current which implies that the corresponding Reynolds numbers typically are in the range from 10^3 to 10^7. This is precisely the range which is covered by the published data sets which are selected. The non-dimensional time-averaged velocity, at different Reynolds number ($Re=3.9\times10^3$, 1.31×10^4, 2.2×10^4, 1.4×10^5), along the center-line of the wake is shown in Fig. 3. The non-dimensional time--averaged stream-wise velocity profiles predicted by different models at various x/d for $Re=3.9\times10^3$ and $Re=1.4\times10^5$ are illustrated in Fig. 4. In addition, the corresponding reference drag coefficients used in the wake models for different Reynolds number are shown in Table .1.

Fig. 3 shows the non-dimensional center-line wake velocity u/U_∞ calculated by the three models versus the horizontal distance x for $y=0$. From Fig. 3-(a) to Fig. 3-(d), it appears that the models tend to have the same asymptotic behavior in the far wake field. The difference is that the Blevins model gives a smaller wake velocity compared with the measured data. This is not unexpected due to that the Blevins model being directly derived from the Reichard model, which already has this kind of limitation in the near wake field. Unlike the Blevins model, the prediction results calculated by the Huse model are slightly larger than those for the Blevins model. This is because the origin in the Huse model is not the same as in the other two models, which assumed that the wake profile is generated by another virtual cylinder in front of the one at the origin. To some degree, this will induce the prediction of the Huse model closer to the physical reality. Actually, the Huse model would inevitably exaggerate the predictions in the near wake domain (approximately when x < *2d*) as indicated in Fig. 3, which would then reduce the model sensitivity during the static riser analysis as discussed in Section 4.2.1 below. In contrast, the results calculated by our proposed model shows a good agreement with the published data, although there is a small deviation for the very near wake domain when Re is comparatively low, e. g. Re = 3900, as shown in Fig. 3-(a). The reason is that at distances less than 2~3 times the diameter of the upstream cylinder, the wake

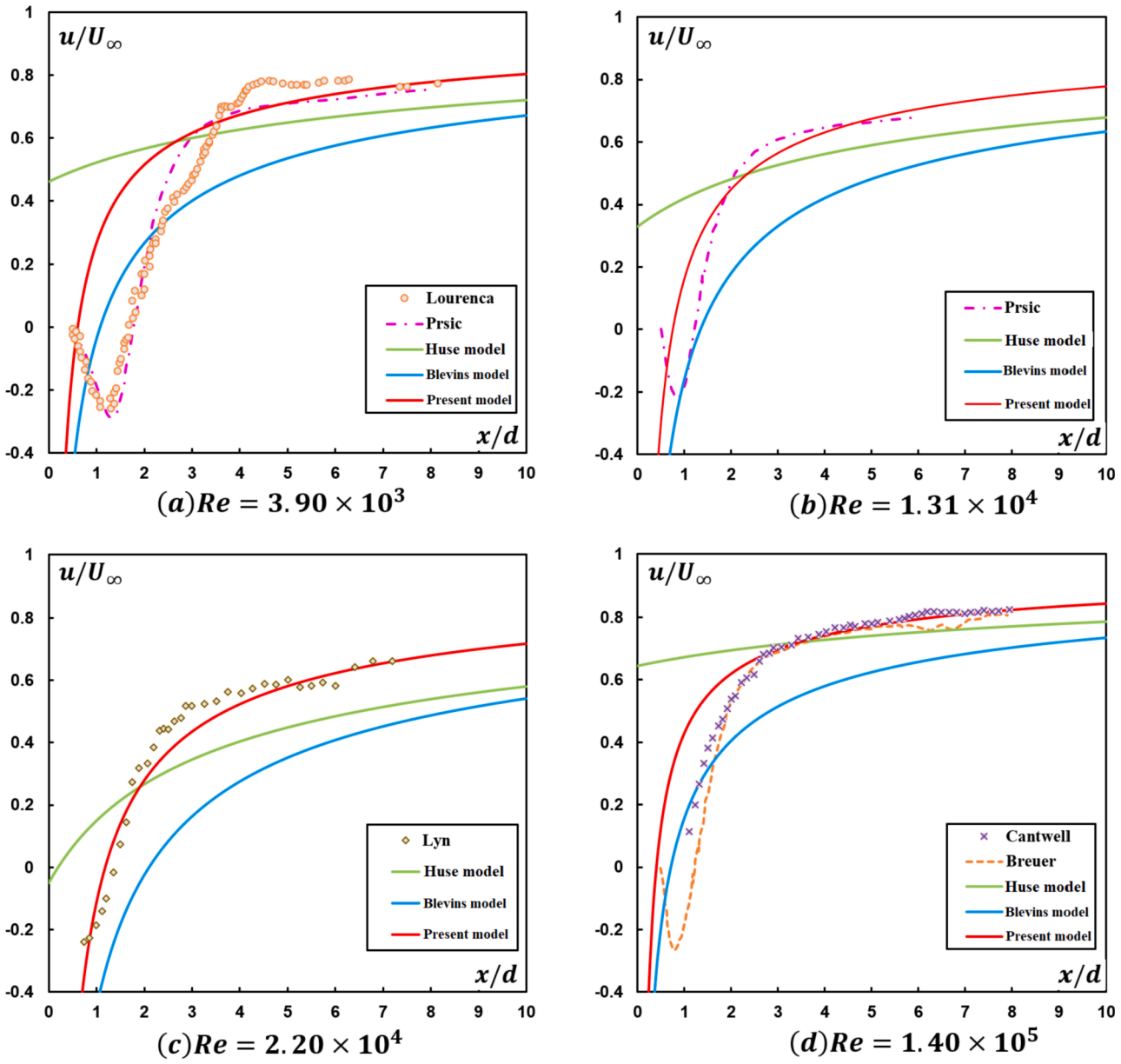

Fig. 3. Development of velocity along the center-line of wake at different Reynolds number.

interference becomes complex with negative suction force involved, which may reduce the accuracy of the model prediction.

Fig. 4 illustrates the non-dimensional stream-wise wake velocity predicted by the three models versus perpendicular distance y/d for different combinations of x/d. From Fig. 4, compared with the CFD results, the Huse model gives a wider wake and larger wake velocity in the near wake field, e.g. $x/d = 1.0 \sim 2.02$, but a wider wake and smaller u/U_∞ when x/d increase to 3~10, which exactly coincide with the feature of the Huse model as illustrated in Fig. 3. Similarly, the Blevins model gives a wider wake and a much smaller local flow velocity. It could be found that the model developed in this study also shows a good agreement with the published CFD data except in the very near wake domain for $Re = 3.9 \times 10^3$.

In general, it can be observed from Figs. 3 and 4 that the wake model proposed in this work is more compatible with the experimental and numerical data compared with the Huse model and the Blevins model. This conclusion particularly applies to the moderate near wake field ($2d \le x \le 10d$).

3. Application of the model

3.1. Force on the downstream riser

The wake velocity distribution can be computed more accurately by using the wake model which was developed in the previous section. However, the problem is that the properties of the wake field vary over the area occupied by the downstream riser. In order to solve this problem (Huse, 1992), the root-mean-square (RMS) value, i.e. $U_{rms}(x, y)$, averaged over the cross-section area of the riser is used for calculating the drag force. The lift force is ignored since the downstream riser is located at the centerline of the wake. This implies that

$$U_{rms}(x,y) = \left\{ \frac{1}{\pi R^2} \int_{-R}^{R} \int_{-\sqrt{R^2-x^2}}^{\sqrt{R^2-x^2}} u^2(x,y)\,dxdy \right\}^{\frac{1}{2}} \tag{18}$$

where R is the radius of the downstream riser.

Therefore, the current force (i.e. the drag force) acting on the unit

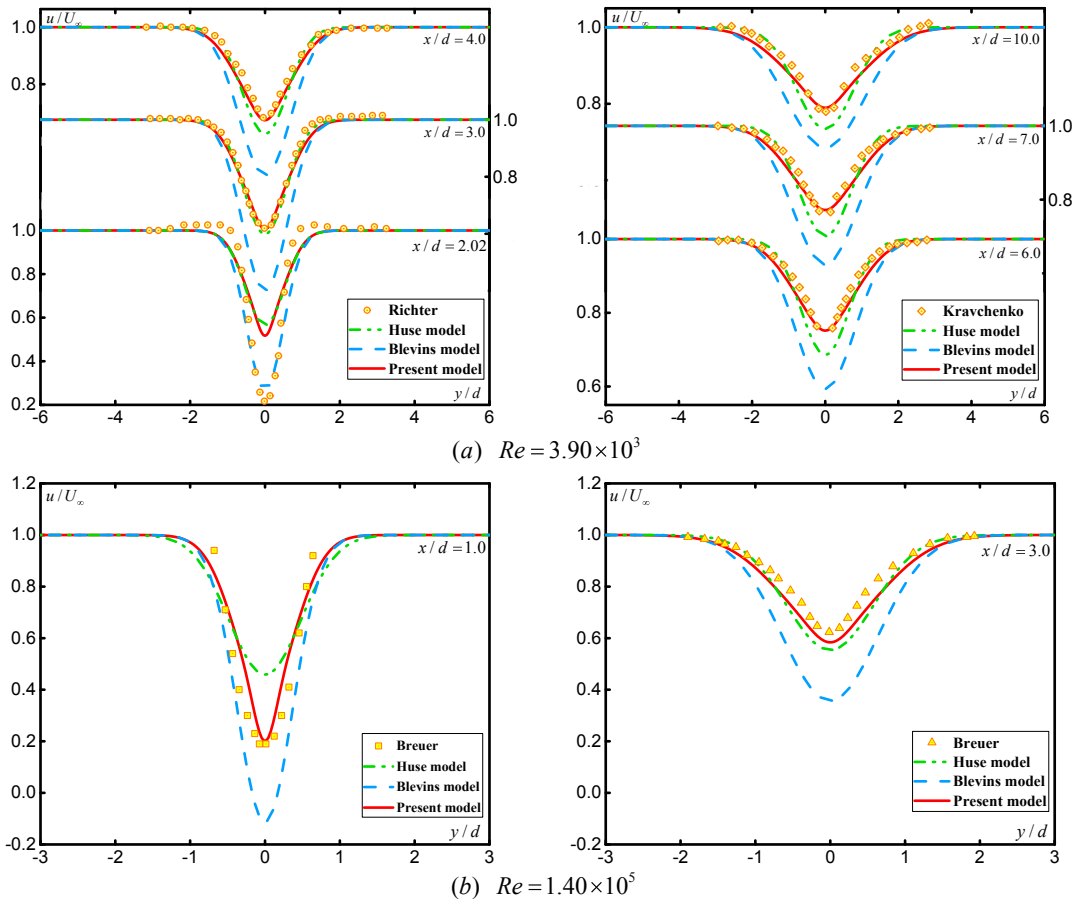

Fig. 4. Stream-wise wake velocity distribution with various x/d at (a) $Re = 3.9 \times 10^3$; (b) $Re = 1.4 \times 10^5$ number.

Table 1
Corresponding drag coefficients for different Reynolds number.

Case	Reynolds number	C_D
Lourenco and Shih (1993)	3.9×10^3	0.99
Prsic et al. (2014)	3.9×10^3	1.0784
Richter et al. (2012)	3.9×10^3	1.0784
Kravchenko and Moin (2000)	3.9×10^3	0.99
Prsic et al. (2014)	1.31×10^4	1.3132
Lyn et al. (1995)	2.2×10^4	2.1
Cantwell and Coles (1983)	1.4×10^5	[1.0, 1.3]
Breuer (2000)	1.4×10^5	[0.712, 1.239]

length of downstream riser can be calculated by the Morison equation as:

$$f_D = \frac{1}{2}\rho \cdot d \cdot C_D \cdot U_{rms}^2 \tag{19}$$

The presented model could also be applied to analysis of the entire riser array analysis by summing the wake contributions from all the upstream risers.

3.2. The mathematical calculation procedure

The static performance of a system comprising two adjacent risers subjected to an uniform current is studied by combining the global riser analysis software Riflex (SINTEF, 2017) with the presented wake model. Riflex is particularly designed to handle static and dynamic analyses of risers and other slender marine structures, but without considering wake effect as part of the flow field representation which is particularly relevant for analysis of riser interferences

It is clearly seen from Eq. (19) that the drag force acting on the downstream riser depends strongly on the RMS wake velocity, which, however, is a function of the distance between the two risers. Hence, the drag force will vary along the downstream riser due to the deformation of the upstream riser and the corresponding altered wake profile. In order to study this effect, the two risers are divided into numerous segments. The downstream wake profile is first established by calculating the relative distance between each pair of riser segments. For the purpose of determining the static equilibrium configuration of the double riser system, a modified iteration procedure (Fu et al., 2017) is hence introduced as follows:

(1) Calculate the vertical downstream wake profile U_{D_i} based on the initial configuration of the double riser system;
(2) Perform a static analysis by updating the downstream wake profile in Riflex and calculated the average distance between each pair of riser segments, i.e. x_i;
(3) Calculate $U_{D_{i+1}}$ according to the new x_i;
(4) Repeat steps 2–3 until a convergent result is obtained.

The entire framework for static analysis is summarized in Fig. 5. The flow field around the upstream riser is assumed to be steady, which implies that it will not be influenced by the deflection of the downstream riser. In addition, the drag coefficients for both risers are taken to be constant in time due to their stable values except for conditions where Reynolds number changes significantly.

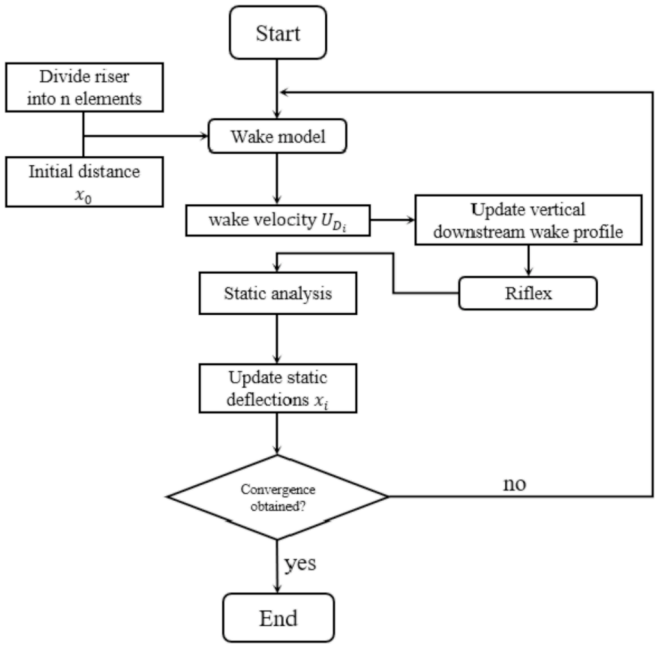

Fig. 5. Flowchart of the proposed calculation procedure.

4. Case study

4.1. Description of riser system

In order to illustrate the analysis procedure, an actual deep-water drilling and producing platform is taken as an example. A system of two adjacent top tensioned risers is considered in the present section, and these are shown in Fig. 6.

Each riser is top tensioned by six tensioners. The water depth is $h = 300m$. The fluid density and the fluid kinematic viscosity is 1025 $g\cdot/cm^3$ and $1.188\times10^{-6}m^2/s$, respectively. A uniform current profile is applied as basis for the analysis. This profile corresponds to a constant velocity throughout the water depth of $h \le 100m$, which is acting in the direction of x-axis. For simplicity, no additional auxiliary components such as attached lines or buoyancy elements are included in the model. Accordingly, both of the risers are modeled as circular steel pipes with constant diameter. Both risers are fixed in translation at both the top and the bottom ends. Detailed properties of each riser are given in Table .2. Sensitivity analyses of the riser displacements are performed with respect to key parameters, such as current velocity U, riser spacing L and riser top tension coefficient T which is defined as $T = Riser\ top\ tension/riser\ total\ submerged\ weight$.

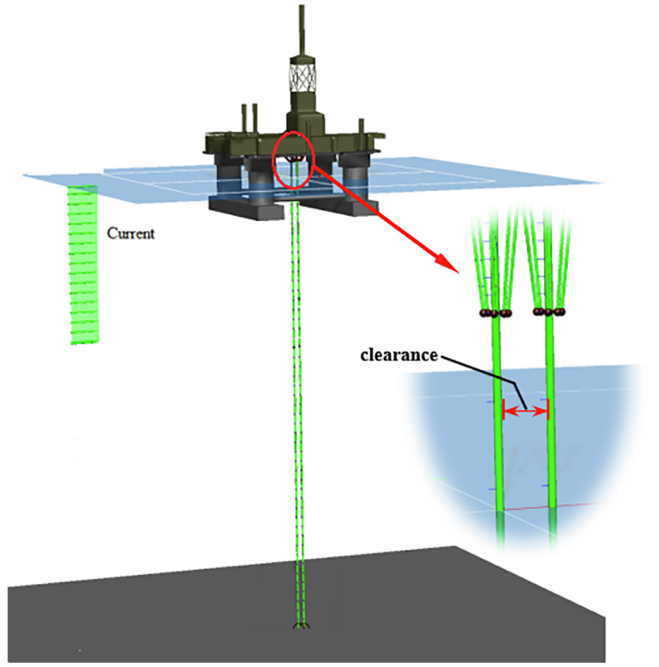

Fig. 6. Model of two top tensioned risers arranged in tandem.

4.2. Results and discussion

The static equilibrium configurations of the two risers are illustrated in Fig. 7 by using different wake models with varying current velocity $U_\infty = 0.7\tilde{}1.25m/s$, varying top tension coefficients $T = 1.2\sim1.8$, and varying initial riser spacing $L = 3.5\sim6.2m$. Comparing to the deformed configuration of the upstream riser, it is seen that the deflection of the downstream riser is significantly decreased due to the effect of the wake interference. Hence, a more accurate and efficient wake prediction model is very important in relation to assessment of riser interference.

4.2.1. Assessment of wake models

Fig. 7-(a) provides a brief comparison of static displacement shapes obtained by using different wake models, which includes the Huse model, the Blevins model and the wake model presented in the present study. The spacing between two risers, which both are top tensioned at a level corresponding to a coefficient of 1.5, is set to be 6.2 m. The environmental current velocity is 1.2 m/s which corresponds to a quite extreme condition. The results calculated by application of Blevins model indicate that this particular combination of riser spacing of $L = 6.2m$ and top tension coefficient of $T = 1.5$ is not safe when subjected to a uniform current of magnitude $U = 1.2$ m/s. However, there is still a sufficiently large distance between the risers when using the other two wake models, even at the most critical water depth of about h = 100 m. Thus, it appears that Blevins model is much more conservative than the other two wake models. The Huse model performs well when the spacing between the risers has a high value or when the magnitude of the current velocity is low. This is due to its particular correction method. Nevertheless, as shown in Fig. 3, the velocities calculated by application of the Huse model are always high even in the very near wake domain, where it should have a low value. This implies that the Huse model is more insensitive in the case of extreme conditions during which collision is about to take place. This poses a potential risk if the design parameters are based on the Huse model. On the contrary, Fig. 3 illustrates that the results calculated by present model are lower than those for the Huse model in the very near domain, while they are a little bit higher when the distance is large. This is exactly what is required, which implies that the present model is more sensitive with respect to finding the critical conditions for riser collision. Consequently, the following three main influencing factors are all studied based on the model presented in the present work.

Table 2
Properties of single risers.

Parameter	Unit	Value
Length	m	326.76
Outside diameter	m	0.324
Inside diameter	m	0.291
Submerged weight	N	1.52×10^5
Riser above water	m	26.76
Young's module	Gpa	210
Poisson ratio	/	0.28
Drag coefficient	/	1.2
Mass coefficient	/	2.0

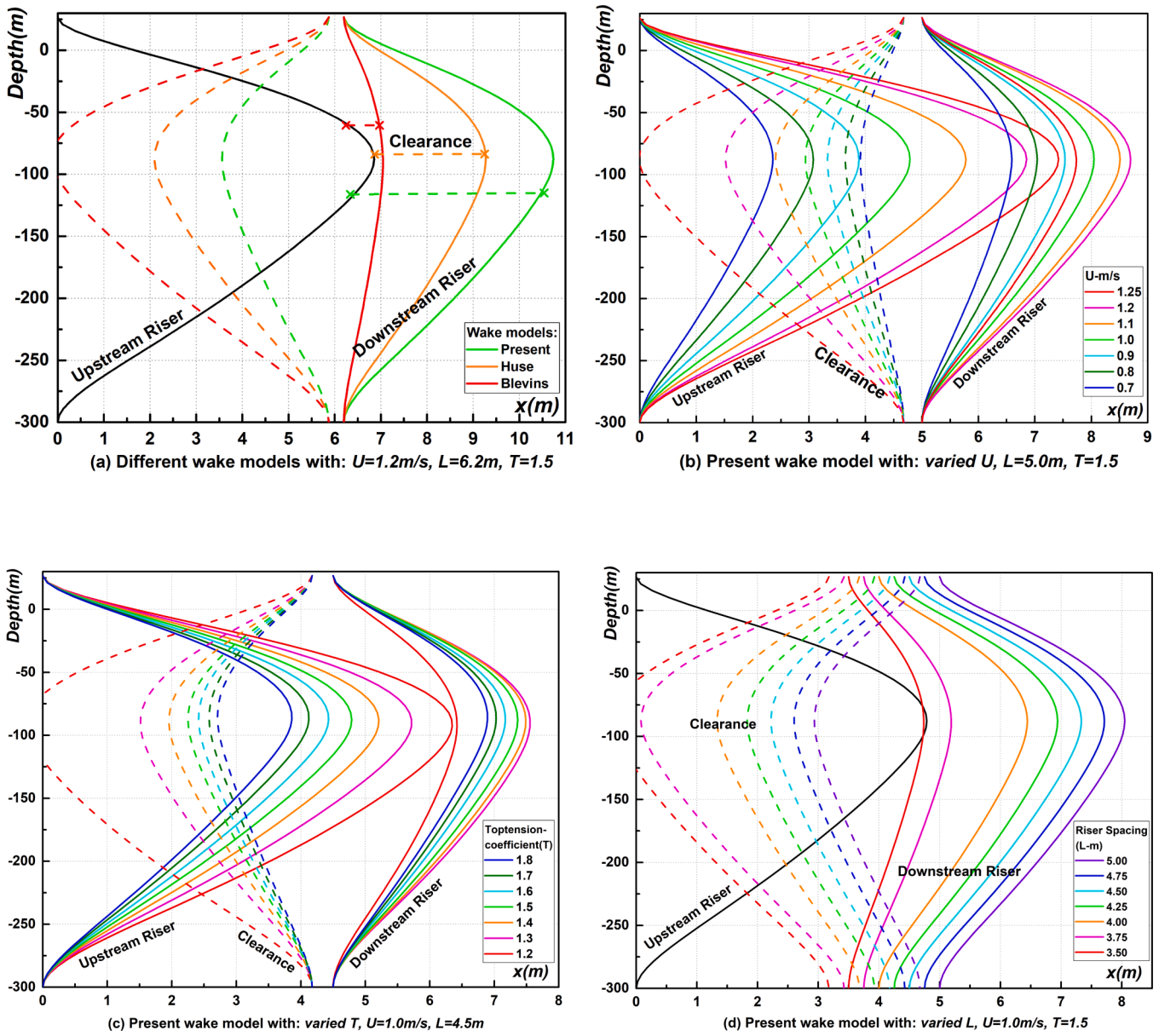

Fig. 7. Static equilibrium deformation of adjacent top tensioned risers in different conditions.

4.2.2. Current velocity

When the riser spacing and other properties are kept constant, then the risk of collision will increase with increasing current velocity. As shown in Fig. 7-(b), the riser spacing and top tension coefficient is set to be $L = 5m$, $T = 1.5$, respectively. The current profile is simplified to a uniform current which increases in magnitude from $U = 0.7$ m/s to $U = 1.25$ m/s. In spite of the static equilibrium deflection for both risers are gradually increasing for increasing current velocity, the increasing amplitude of the upstream riser is evidently larger than the downstream one. This will continuously reduce the minimum clearance between two risers until contact between the risers takes place. The critical current velocity is approximately equal to 1.25 m/s with this particular combination of riser spacing and top tension coefficient. The current velocity has a great impact on the riser clearance, but this is a parameter which is given by the environment and as basically beyond the control of the designers or operators (once a particular site has been selected).

4.2.3. Riser top tension

In order to find the critical top tension coefficient, the current velocity and the initial riser spacing are kept constant, with $U = 1.0$ m/s *and* $L = 4.5m$. The top tension coefficient is then reduced from 1.8 to 1.2 step by step, and the results from the calculations are shown in Fig. 7-(c). Generally, it appears that the top tension has a great influence on the upstream riser. The clearance between the two risers is evidently decreasing when reducing the top tension coefficient. Finally, the collision may occur when top tension coefficient goes down to 1.2. The top tension coefficient is a more "flexible" design parameter than riser spacing, and it can be changed manually during the process of drilling or production.

However, a too high top tension may overload the tensioner system, as well as the riser itself due to the associated high stresses.

4.2.4. Riser spacing

In order to find the critical riser spacing, the current velocity and the top tension coefficient are kept constant, *with* $U = 1.0$ m/s and $T = 1.5$, while the riser spacing is reduced from 5.0 m step by step. The results of the calculations are shown in Fig. 7-(d). It can be observed that the deformation of the downstream riser decreases significantly when the

riser spacing is reduced. Of course, the corresponding clearance variation clearly exhibits the same trend. For the present conditions, the critical riser spacing is found to be closer to 3.5 m. Riser spacing is one of the most important design parameters for drilling or producing platform systems. Riser collision can be efficiently prevented by increasing the riser spacing. Nevertheless, it should be noticed that increasing the riser spacing directly means increasing the size of the wellbay which will result in significant cost penalties.

5. Conclusions

Consideration of wake interference is of great significance for the static analysis of riser interaction and potential for collision. In the present work, static deflections of two top tensioned marine risers arranged in tandem are investigated. A new effective wake model for circular cylinders is developed based on solving Prandtl's boundary-layer equations by using the Tollmien's first approximation method and the Goldstein's second approximation method.

Comparison of the results among the three models indicates that the local flow velocity in the near wake domain will be over-estimated by the Huse model but underestimated by the Blevins model. Hence, the Huse model is relatively insensitive in this domain and Blevins model tend to be conservative. It is demonstrated that the new model proposed in this work has a good stability and reliability when predicting the wake profile in the critical Reynolds region. This applies in particular when it is applied to calculate the critical conditions associated with riser collision problems.

For the 'No Collision Allowed' strategy, a calculation procedure is presented which enables determination of the pairwise static equilibrium configuration of risers by combining the global riser analysis software Riflex and the new wake model. Our analysis through a case study shows that the both the riser-spacing and the top tension coefficient have a significant influence on the likelihood of riser interference. Therefore, optimal combination of these two parameters should primarily be considered in order to avoid riser collision.

It should be noted here that although an improved analytical wake model is proposed on this study, in the future a development of some type of optimization procedure for the very near wake domain ($x < 2d$) would be beneficial. An accurate estimation of the transverse flow velocity for predicting the lift force on the staggered arranged downstream riser has to be provided and is also planned as part of future work.

Acknowledgments

The authors gratefully acknowledge financial support from "the National Natural Science Foundation of China" with fund number 51874326 and 51574261 and "the National Major Science and Technology Projects of China" with fund number 2016ZX05020-006-005.

Appendix A

The solution process for the first deficit velocity can be described as follows:

Following Prandtl's shear stress hypothesis, the laminar kinematic viscosity υ in Eq. (12) can be replaced by the virtual kinematic viscosity $\varepsilon_\tau = \kappa_1 u_{1max} b$ which can be regarded as an unknown constant ε_0. Consequently, Eq. (12) can be written as:

$$\begin{cases} -\dfrac{\partial \overline{u}_1}{\partial x} + \dfrac{\partial v_1}{\partial y} = 0 \\ U_\infty \dfrac{\partial \overline{u}_1}{\partial x} = \varepsilon_o \dfrac{\partial^2 \overline{u}_1}{\partial y^2} \end{cases} \tag{A-1}$$

In addition, the first term of deficit velocity $\overline{u}_1$ is assumed of the form:

$$\begin{cases} \overline{u}_1 = U_\infty \cdot C \cdot \left(\dfrac{x}{d}\right)^{-1/2} g(\eta) \\ \eta = y\sqrt{\dfrac{U_\infty}{\varepsilon_o x}} \end{cases} \tag{A-2}$$

Inserting Eq. (A-2) into Eq. (A-1), and further, integrating it twice gives the solution:

$$g(\eta) = exp\left(-\frac{1}{4}\eta^2\right) \tag{A-3}$$

The drag force due to the velocity profile in the wake can be calculated by integrating the momentum equation:

$$F_D = \rho h \int_{-\infty}^{+\infty} u \cdot (U_\infty - u)\, dy \tag{A-4}$$

where the quadratic and higher terms of u_1 are neglected.

The drag force can also be obtained from the Morison Equation:

$$F_D = \frac{1}{2}\rho \cdot h \cdot d \cdot C_D \cdot U_\infty^2 \tag{A-5}$$

where C_D is the drag coefficient.

The constant C in Eq. (A-2) is then determined combining Eq. (A-4) with Eq. (A-5), and becomes:

$$C = \frac{C_D}{4\sqrt{\pi}}\sqrt{\frac{U_\infty d}{\varepsilon_o}} \tag{A-6}$$

Consequently, the form of $\overline{u}_1$ is:

$$\begin{cases} \dfrac{\overline{u}_1}{U_\infty} = \alpha \times C_D^{1/2} \cdot \left(\dfrac{x}{d}\right)^{-1/2} \cdot exp\left(-4\pi\alpha^2\zeta^2\right) \\ \alpha = \dfrac{1}{4\sqrt{\pi}}\sqrt{\dfrac{U_\infty C_D d}{\varepsilon_o}}, \quad \zeta = C_D^{-1/2} \cdot \left(\dfrac{x}{d}\right)^{-1/2} \cdot \left(\dfrac{y}{d}\right) \end{cases} \tag{A-7}$$

Furthermore, the first component of the transverse velocity is also obtained as:

$$\begin{cases} \dfrac{v_1}{U_\infty} = -\sqrt{4\pi} \cdot \alpha^2 \cdot x^{-1/2} \cdot C_D^{1/2} \cdot \zeta \times exp\left(-4\pi\alpha^2\zeta^2\right) \\ \alpha = \dfrac{1}{4\sqrt{\pi}}\sqrt{\dfrac{U_\infty C_D d}{\varepsilon_o}}, \quad \zeta = C_D^{-1/2} \cdot \left(\dfrac{x}{d}\right)^{-1/2} \cdot \left(\dfrac{y}{d}\right) \end{cases} \tag{A-8}$$

In the investigation of H. Schlichting (1979), $\varepsilon_0/(U_\infty C_D d)$ was empirically set to be 0.022. In the present paper, a dimensionless parameter α is introduced in place of the empirical item.

Based on this, the first term of the deficit velocity is then given by:

$$\frac{\overline{u}_1}{U_\infty} = \alpha \cdot C_D^{1/2} \cdot \left(\frac{x}{d}\right)^{-1/2} \cdot exp\left\{-4\pi\alpha^2 \cdot C_D^{-1} \cdot \left(\frac{x}{d}\right)^{-1} \cdot \left(\frac{y}{d}\right)^2\right\} \tag{A-9}$$

Appendix B

The solution process in order to find the second deficit velocity can be described as follows:

Substituting $\overline{u}_1$ and $\overline{v}_1$, which are obtained from Appendix A, into Eq. (15), it is found that $\overline{u}_2$ satisfies the following equation:

$$-U_\infty \frac{\partial \overline{u}_2}{\partial x} + \varepsilon_o \frac{\partial^2 \overline{u}_2}{\partial y^2} = \frac{\alpha^2}{2x} C_D \left(\frac{x}{d}\right)^{-1} exp\left(-8\pi\alpha^2\zeta^2\right) \tag{B-1}$$

To solve this equation, the second term of the deficit velocity $\overline{u}_2$ is assumed to be of the form:

$$\frac{\overline{u}_2}{U_\infty} = \frac{\sqrt{8} \cdot \alpha \cdot \zeta}{x} exp\left(-4\pi\alpha^2\zeta^2\right) h(\zeta) \tag{B-2}$$

Inserting Eq. (B-2) into Eq. (B-1), and then, integrating the differential equation twice we obtain:

$$\frac{\overline{u}_2}{U_\infty} \approx \frac{\alpha^2}{2} \cdot C_D \cdot \left(\frac{x}{d}\right)^{-1} \cdot exp\left(-4\pi\alpha^2 \cdot \beta \cdot \zeta^2\right) \tag{B-3}$$

where β is another dimensionless coefficient like α.

References

Assi, G.R.S., Meneghini, J.R., Aranha, J.A.P., Bearman, P.W., Casaprima, E., 2006. Experimental investigation of flow-induced vibration interference between two circular cylinders. J. Fluids Struct. 22, 819–827. https://doi.org/10.1016/j.jfluidstructs.2006.04.013.

Blevins, R.D., 2005. Forces on and stability of a cylinder in a wake. J. Offshore Mech. Arct. Eng. 127 https://doi.org/10.1115/1.1854697.

Breuer, M., 2000. A challenging test case for large eddy simulation: high Reynolds number circular cylinder flow. Int. J. Heat Fluid Flow 21, 648–654. https://doi.org/10.1016/S0142-727X(00)00056-4.

Cantwell, B., Coles, D., 1983. An experimental study of entrainment and transport in the turbulent near wake of a circular cylinder. J. Fluid Mech. 136, 321–374. https://doi.org/10.1017/S0022112083002189.

DNV-RP-F203, 2009. Offshore Standard Dmv-Rp-F203:riser Interference. Det Norske Veritas Norway.

Fu, P., Leira, B.J., Myrhaug, D., 2017. Reliability analysis of wake-induced collision of flexible risers. Appl. Ocean Res. 62, 49–56. https://doi.org/10.1016/j.apor.2016.11.001.

Fu, P., Leira, B.J., Myrhaug, D., 2018. The effect of local wake model on collision probability for risers subjected to current and random waves. Ocean Eng. 162, 331–340. https://doi.org/10.1016/j.oceaneng.2018.04.099.

Goldstein, S., 1933. On the two-dimensional steady flow of a viscous fluid behind a solid body. Proc. R. Soc. Lond. 142, 545–562. https://doi.org/10.1098/rspa.1933.0187.

Huang, S., 2010. Instability of a vertical riser in the wake of an upstream vertical riser. Appl. Ocean Res. 32, 351–357. https://doi.org/10.1016/j.apor.2009.12.001.

Huse, E., 1992. Current force on individual elements of riser arrays. IEEE Trans. Ind. Appl. 132, 35–57. https://www.onepetro.org/conference-paper/ISOPE-I-92-135.

Huse, E., Muren, P., 1987. Drag in Oscillatory Flow Interpreted from Wake Considerations. Offshore Technology Conference, Houston, Texas, pp. 135–142.

Kang, S., 2003. Characteristics of flow over two circular cylinders in a side-by-side arrangement at low Reynolds numbers. Phys. Fluids 15, 2486–2498. https://doi.org/10.1063/1.1596412.

Kravchenko, A.G., Moin, P., 2000. Numerical studies of flow over a circular cylinder at Re D= 3900. Phys. Fluids 12 (2), 403–417. https://doi.org/10.1063/1.870318.

Lourenco, L., Shih, C., 1993. Characteristics of the plane turbulent near wake of a circular cylinder: a particle image velocity study (private communication), reported by Kravchenko, AG, Moin, P., 2000. Numerical studies of flow over a circular cylinder at ReD= 3900. Phys. Fluids 12, 403–417. https://doi.org/10.1063/1.870318.

Lyn, D.A., Einav, S., Rodi, W., Park, J.H., 1995. A laser-Doppler velocimetry study of ensemble-averaged characteristics of the turbulent near wake of a square cylinder. J. Fluid Mech. 304, 285–319. https://doi.org/10.1017/S0022112095004435.

Price, S.J., 1975. Wake induced flutter of power transmission conductors. J. Sound Vib. 38, 125–147. https://doi.org/10.1016/S0022-460X(75)80023-X.

Price, S.J., Paidoussis, M.P., 1984. The aerodynamic forces acting on groups of two and three circular cylinders when subject to a cross-flow. J. Wind Eng. Ind. Aerodyn. 17, 329–347. https://doi.org/10.1016/0167-6105(84)90024-2.

Prsic, M.A., Ong, M.C., Pettersen, B., Myrhaug, D., 2014. Large Eddy Simulations of flow around a smooth circular cylinder in a uniform current in the subcritical flow regime. Ocean Eng. 77, 61–73. https://doi.org/10.1016/j.oceaneng.2013.10.018.

Reichardt, H., 1941. Über eine neue Theorie der freien Turbulenz. ZAMM-Journal of Applied Mathematics and Mechanics/Zeitschrift für Angewandte Mathematik und Mechanik 21. In: Boundary-Layer Theory. McGraw-Hill, pp. 257–264. Reported by Schlichting, H., Gersten, K., 1979.

Richter, D., Iaccarino, G., Shaqfeh, E.S., 2012. Effects of viscoelasticity in the high Reynolds number cylinder wake. J. Fluid Mech. 693, 297–318. https://doi.org/10.1017/jfm.2011.531.

Sagatun, S.I., Herfjord, K., Holmås, T., 2002. Dynamic simulation of marine risers moving relative to each other due to vortex and wake effects. J. Fluids Struct. 16, 375–390. https://doi.org/10.1006/jfls.2001.0424.

Schlichting, H., Gersten, K., 1979. Boundary-Layer Theory. McGraw-Hill.

SINTEF, O., 2017. RIFLEX 4.10. 1 User Guide. SINTEF Ocean: Trondheim, Norway.

Sumner, D., 2010. Two circular cylinders in cross-flow: a review. J. Fluids Struct. 26, 849–899. https://doi.org/10.1016/j.jfluidstructs.2010.07.001.
Sumner, D., Wong, S.S.T., Price, S.J., Paıdoussis, M.P., 1999. Fluid behaviour of side-by-side circular cylinders in steady cross-flow. J. Fluids Struct. 13, 309–338. https://doi.org/10.1006/jfls.1999.0205.
Tollmien, W., Miner, D.M., 1931. The Production of Turbulence. National advisory committee for aeronautics langley field va langley aeronautical laboratory.
Wu, W., Huang, S., Barltrop, N., 2002. Current induced instability of two circular cylinders. Appl. Ocean Res. 24, 287–297. https://doi.org/10.1016/S0141-1187(03)00003-8.
Zdravkovich, M.M., 1987. The effects of interference between circular cylinders in cross flow. J. Fluids Struct. 1, 239–261. https://doi.org/10.1016/S0889-9746(87)90355-0.